Rock Dynamics – Experiments, Theories and Applications – Li, Li & Zhang (Eds)
© 2018 Aydan, Ito & Ito, ISBN 978-0-8153-9667-3

Dynamic response of support systems during the excavation of underground openings

Ö. Aydan
University of Ryukyus, Okinawa, Japan

F. Ito
Taisei Corporation, Tokyo, Japan

T. Ito
Toyota National College of Technology, Toyota, Japan

ABSTRACT: Rockburst, earthquake and blasting causes some dynamic loads on rock support and rock reinforcement. Members of rock support and rock reinforcement are generally made of steel bar or cables, which are resistant against corrosion. These support members may be subjected vibrations induced by turbines, vehicle traffic and long-term corrosion in addition to dynamic loading due to earthquakes, rockburst and blasting. The authors carried out some theoretical, numerical and experimental studies on rockbolts and rock-anchors under shaking and impulsive loading. In this study, the authors present the outcomes of these studies and discuss their practical implications.

1 INTRODUCTION

Dynamic problems such as rockburst, earthquake and blasting causes some dynamic loads on rock support and rock reinforcement. Rockbolts and rock anchors are commonly used as principal reinforcement members in underground and surface excavations while shotcrete and concrete lining are used as support members. Rockbolts and rock anchors are generally made of steel bar or cables, which are resistant against corrosion. These support members may be subjected earthquake loading, vibrations induced by turbines, vehicle traffic and long-term corrosion. Figure 1 shows the cable rock anchors used at a rock slope ruptured during the 2008 Iwata-Miyagi earthquake (Aydan 2017, 2018).

Figure 2 shows the state of rock anchors and rockbolts at underground excavations experienced rockburst and spalling problems. The authors present some theoretical, numerical and experimental studies on rockbolts and rock-anchors under shaking and impulsive loading in this study. Furthermore, they discuss their practical implications.

Figure 1. Rock anchors ruptured by the 2008 Iwate-Miyagi earthquake (from Aydan 2017, 2018).

Figure 2. The state of rock anchors and rockbolts at underground excavations experienced rockburst and spalling problems (arranged from Aydan 2018).

2 EXPERIMENTAL STUDIES

2.1 *Response on acrylic rockbolt under impulsive Load*

It is very rare to see any discussion or experimental result on the load-displacement-time or stress-strain-time responses under impulsive loads except by Aydan (2017, 2018). Aydan (2017, 2018) devised an experimental set-up for this purpose. The experimental set-up consists of an acrylic bar attached with strain gauge and fixed to a support at top as illustrated in Figure 3. The diameter and length of the acrylic bar were 8 mm and 200 mm respectively. An object with a given weight was instantaneously applied to the lower end of the bar. The strain

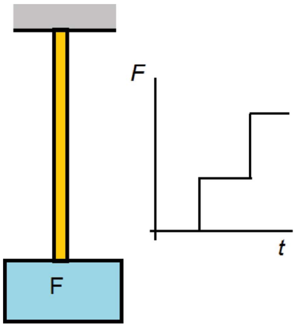

Figure 3. Schematic illustration of the experimental set-up.

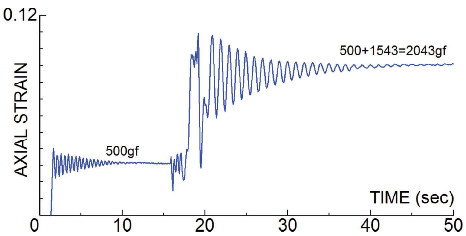

Figure 4. Strain response of an acrylic bar subjected by the weight of an object.

response was monitored using WE7000 dynamic data acquisition system with a sampling interval of 10 ms. In the first stage, 500 gf was applied and then load was increased by 1543 gf. Figure 4 shows the strain variation with time. As noted from the figure, the strain fluctuates and become asymptotic to the static strain level for the applied stress level. Although the experiment is quite simple, it clearly shows that the loading of samples and structures as well as excavation of rock engineering structures should be treated as a dynamic phenomenon.

2.2 *Model tests on fully grouted rockbolts against sliding*

Owada and Aydan (2005) carried out some model experiments on the development of axial forces grouted rockbolts stabilizing the potentially unstable blocks in sidewalls of the underground openings or rock slopes subjected to planar sliding as shown in Figure 5 using shaking tables. An acrylic bolt equipped with three strain gauges shown in Figure 6 was used and the inclination of the bolt was varied as 45, 90 and 135 degrees with respect to sliding plane, which is inclined at an angle of 45 degrees to the horizontal. Strain gauge numbered 2 (St2) is set next to the discontinuity plane. The dynamic response of the acrylic bolt under impulsive gravity loading has been already shown in Figure 4. The samples with different orientation of model rockbolt were also tested under static loading condition and the experimental results are shown in Figures 7 and 8.

As noted, reinforcement effect differs depending upon the installation angle of rockbolts. Figures 7 and 8 also imply that the peak resistance is mobilized when the angle between the bolt axis and the

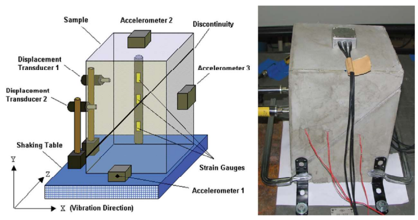

Figure 5. An illustration of the experimental set-up and its view.

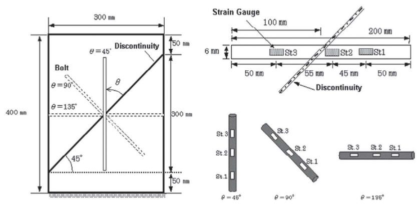

Figure 6. A drawing of an instrumented sample and position of strain gauges.

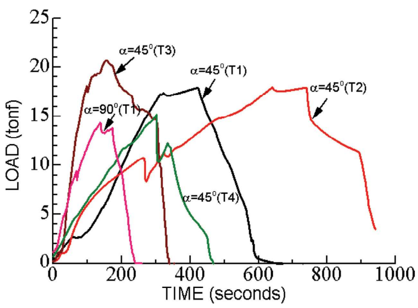

Figure 7. The load response of samples bolted having different orientations.

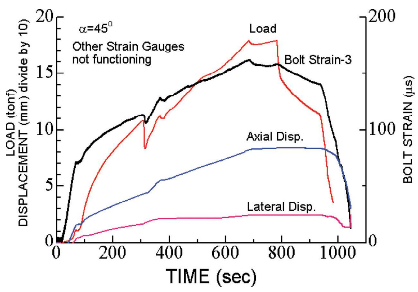

Figure 8. Load, strain and displacement responses of a sample with 45 degrees rockbolt.

sliding movement is 45 degrees. On the other hand, the peak resistance is lower and the amount of slip is larger when the angle between the bolt axis and the sliding movement is 90 degrees.

Figures 9–11 show the applied base acceleration and strains in the bolt and displacement of the potentially unstable block. As noted from the figures, some residual strains occur in the bolts following the termination of shaking. Similarly, the block is displaced permanently. Strain at Gauge 2 is always largest as expected. Although the measured strain levels are small as compared with their yield strain level, the permanent straining results from the permanent displacement of the potentially unstable block.

As shown in Figure 12, the amplitude of acceleration is increased step wise up to 450 gals. When the acceleration was less than 200 gals, the straining of the bolt and displacement of the potentially unstable block was small. However, strains and permanent displacement become larger after each acceleration level increment.

2.3 *Planar sliding of rock slope and sidewall models*

A shaking table was used while changing the configuration of model in order to study the planar sliding of rock slopes. Figure 13 shows a typical experimental set-up. The block was 137 mm high, 137 mm wide and 37 mm thick. A plane of discontinuity with an inclination of 58° was introduced into the block. The friction angle of the saw-cut surface was measured by tilting test and its value ranged between 24–26°. Two springs with a length

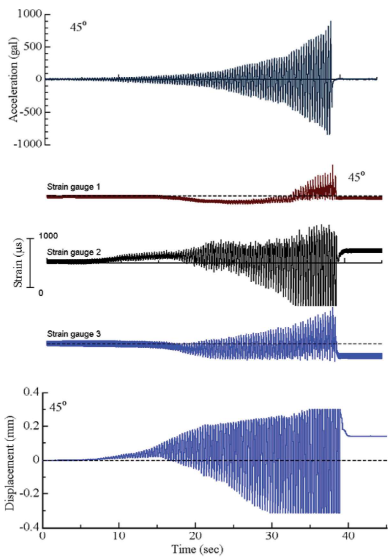

Figure 9. The responses of bolt strains and displacement of unstable block in relation to applied base acceleration (bolt angle 45°).

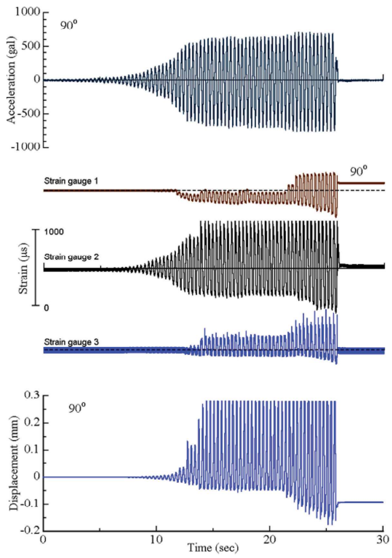

Figure 10. The responses of bolt strains and displacement of unstable block in relation to applied base acceleration (bolt angle 90°).

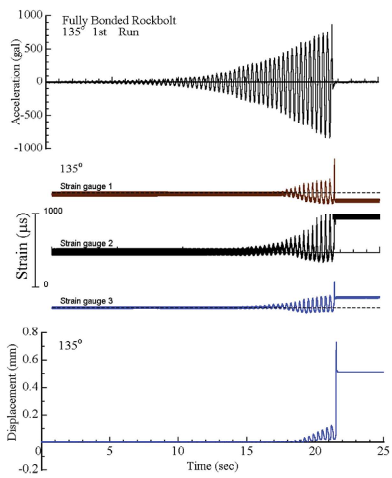

Figure 11. The responses of bolt strains and displacement of unstable block in relation to applied base acceleration (bolt angle 45°).

of 30 mm as the models rockbolts and rock anchors of end-anchored type were fixed at the both sides of the block so that the springs cross the potential sliding surface as shown in Figure 13.

The dead weight of the potentially unstable block was 69.7 gf and a surcharge load of 172.7 gf was imposed on the potentially unstable block. The block was unstable without springs due to the high inclination angle of the sliding plane.

More than 4 experiments were performed. As the results are quite similar to each other, two examples are described herein. The model conditions are fun-

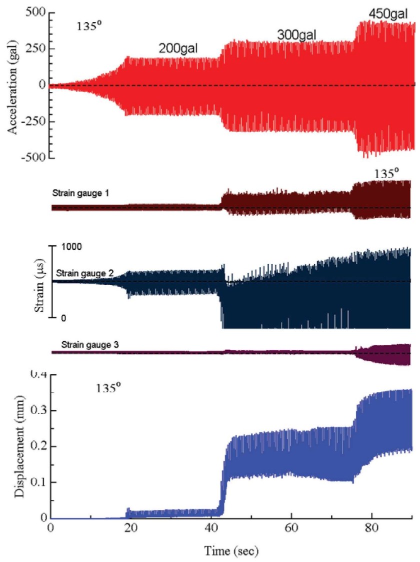

Figure 12. The responses of bolt strains and displacement of unstable block in relation to applied base acceleration (bolt angle 135°).

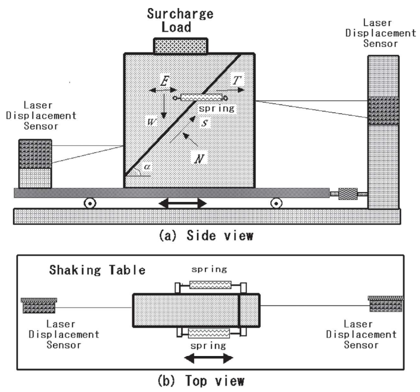

Figure 13. The experimental set-up for model tests.

damentally the same. The only difference is the level and pattern of the acceleration form imposed on the models. Figures 14 and 15 show the acceleration responses. In *Rockbolt Experiment 3*, the maximum base acceleration was 390 gal while it was 590 gal in *Rockbolt Experiment 4*. As a result, the ultimate displacement, ultimate bolt-force and cumulative AE become higher for the model subjected to higher acceleration levels. During each increase of acceleration level, the displacement and bolt-force and cumulative AE increase simultaneously. As the acceleration level becomes stationary, the responses of all parameters tend to become stationary. This is a quite natural result, as the bolt-force on the sliding plane becomes larger after each cycle and this increases the resistance of the plane against sliding.

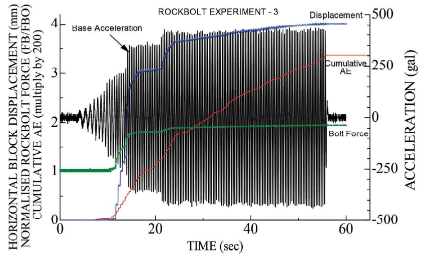

Figure 14. Measured responses of displacement, bolt-force, cumulative AE and imposed base acceleration.

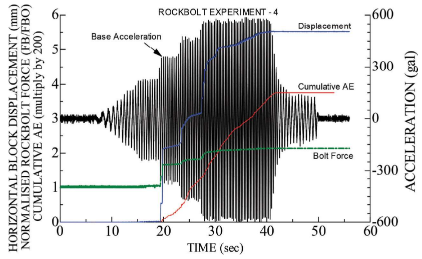

Figure 15. Measured responses of displacement, bolt-force, cumulative AE and imposed base acceleration.

Finally, the bolt-force becomes large enough to stop the sliding of the block, if it does not fail. These two simple yet very meaningful experiments clearly demonstrate that the bolts and anchors used as a part of the support system may experience greater load levels than that at the time their installation after each passage of dynamic loads. This outcome has very important implications that support systems may fail during their service lives not due to their deterioration but also cyclic loads resulting from different causes as mentioned in the introduction.

3 NUMERICAL ANALYSES

3.1 *Rockbolt subjected to impulsive load*

A numerical experiment on the response of 2 m long point anchored steel rockbolt with a diameter of 25 mm was analysed using a dynamic finite element method developed by the author (Aydan 2004). The model was subjected to impulsive rock load of 25 kN and the numerical model is fundamentally similar to the experimental set-up shown in Figure 3 except the size of rockbolt and magnitude of the load. The rockbolt was assumed to be visco-elastic of Voigt-Kelvin type with a viscosity coefficient of 10 MPa·s and elastic modulus of 200 GPa. Figure 16 shows the displacement responses of the steel rockbolt at selected distances from the fixed-end. After about 10 ms, the displacement responses of the steel rockbolt converge to those obtained from the static solution. If the rockbolt is purely elastic, the head of the rockbolt response would show a cyclic displacement behaviour as shown in Figure 17. As noted in the experiment, every material in nature has some viscous resistance so that the displacement of rockbolts eventually converges to those measured under static condition.

Figure 18 shows the response of the axial stress in the rockbolt for the displacement response shown in Figures 16 and 17. The axial stress in the rockbolt several times that under static condition. This result is fundamentally similar to that shown in Figure 4. The experiment and numerical experiment clearly illustrate that the rockbolts may experience loads under dynamic condition several times of those under static condition.

3.2 *Rockbolt response during excavation*

A circular underground opening at a depth of 100 m was assumed to be reinforced by rockbolts of 4 m long with a 25 mm diameter installed in a hole with a radius of 36 mm. The spacing of rockbolts with an elastic modulus of 200 GPa were assumed to be 1 m by 1 m. The elastic modulus and Poisson's ratio of rock mass were 3 GPa and 0.25, respectively. Figure 19 shows the radial and tangential stresses normalized by the in-situ stress at a distance of 25 cm from the opening surface. It is interesting to note that the radial and tangential stresses are less than those of unsupported case, which indicates the reinforcement effect of rockbolts through the internal pressure as well as shear interaction between rockbolts and surrounding ground.

Figure 20 shows the variation of axial stress in the rockbolts at selected distance from the head of the rockbolts. The overall response of axial stress in rockbolts are quite similar to the changes of the stresses in rock mass. One of important observations is that the axial stress in rockbolts would fluctuate and they would experience larger axial stresses than those under static condition.

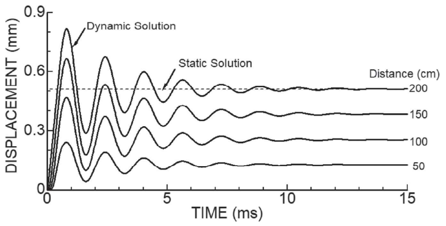

Figure 16. Displacement responses of the rockbolt at selected distances from the fixed-end.

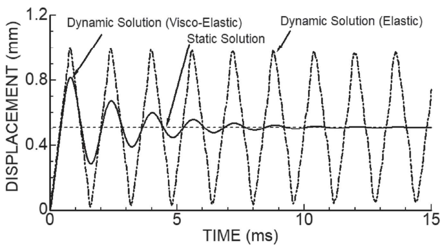

Figure 17. Comparison of displacement responses of the rockbolt head for elastic and visco-elastic condition.

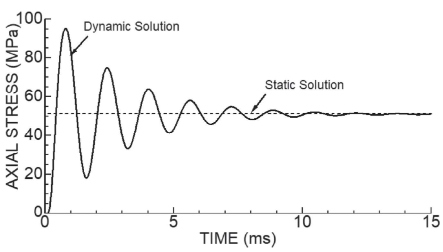

Figure 18. Comparison of axial stress of the rockbolt head for dynamic and static conditions.

3.3 *Response of rock anchors of a power house subjected to turbine-induced vibration*

Rock mass generally contains geological discontinuities and these discontinuities play major role on the local instabilities in underground openings (i.e.

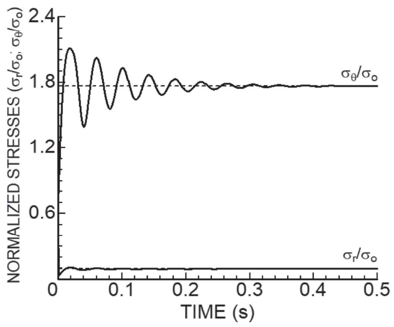

Figure 19. Variation of radial and tangential stresses in rock mass at a distance of 25 cm from the opening perimeter for bolted case.

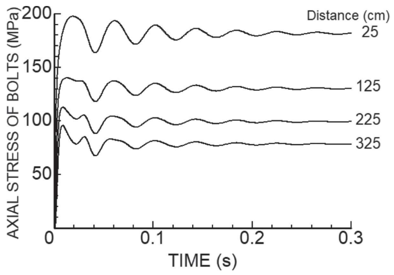

Figure 20. Variation of axial stress in rockbolts at a distance of 25 cm from the opening perimeter for bolted case.

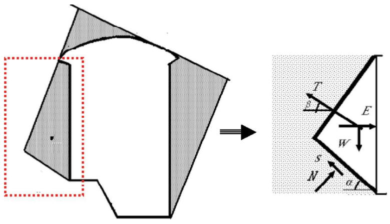

Figure 21. Identified unstable blocks and force equilibrium conditions.

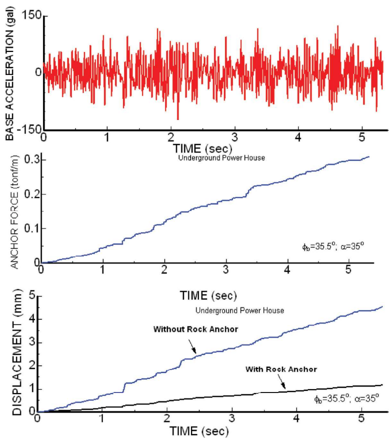

Figure 22. Computed displacement and axial force responses.

Aydan 1989, Kawamoto et al. 1991). The potentially unstable blocks were identified around an underground cavern shown in Figure 10.30 on the basis of in-situ investigations as well as geological investigations during the construction phase (Aydan, 2016, Aydan et al. 2012).

The axial force T of rock anchors is also computed from a relation similar to Eq. 1, given below:

$$T = C\delta^{b} \tag{1}$$

The displacement of rock anchors induced by the relative displacement during each relative motion due to sliding was computed from geometrical considerations. It should be also noted that there is no sliding if the rock anchor force attains a certain level. Furthermore, the oscillations of anchor force due to visco-elastic response during each increment of axial force were neglected in computations.

Figure 22 shows the computational results for the block shown in Figure 21 for two different situations using the induced radial vibration record at the penstock. In the first case, no rock anchors were considered while rock anchors were assumed to be installed in the second case. The inclination of discontinuity was set to 35o and its friction coefficient was determined from tilting tests as 35.5o. When no rock anchors are installed, the block tends to slide downward when vibrations induced are sufficient to cause sliding. However, the relative sliding movements of the block is restricted and the amount of sliding becomes less and the anchor force tends to become asymptotic to a certain level for the given amplitude of vibrations. This computational result also implied that the axial forces may increase during their service life when forces resulting from vibrations in the vicinity of cavern and/or earthquakes from time to time. These increases may also lead to the rupture of rock anchors in long-term besides the reduction of cross sections of rock anchors due to corrosion.

4 CONCLUSIONS

Some experiments on dynamic response of point-anchored rockbolt model under impulsive load are described. The axial strain of the model rock-anchor fluctuated and became asymptotic to the static strain level for the applied stress level.

Some model experiments were carried out on the development of axial forces in rock anchors and grouted rockbolts, stabilizing the potentially unstable blocks in sidewalls of the underground openings using shaking. Experiments showed that the anchor force increased after each slip event in a step-like fashion and becomes asymptotic to a certain value thereafter. Furthermore, the block does not return to its original position, implying that the axial force becomes higher than the applied pre-stress level following each slip event. The numerical experiments also clearly illustrated that the rockbolts may experience loads under dynamic condition several times of those under static condition.

An actual excavation of a circular tunnel supported by rockbolts was considered as a dynamic problem under hydrostatic *in situ* stress condition. The comparisons of stresses induced for unbolted and bolted cases indicated that the radial and tangential stresses are less than those of the unsupported case, which indicates the reinforcement effect of rockbolts through the internal pressure as well as shear interaction between rockbolts and surrounding ground.

REFERENCES

Aydan, Ö. 1989. *Reinforcement of rock engineering structures*. PhD Thesis, Nagoya University.

Aydan, Ö. 2017. *Rock dynamics*. CRC Press, ISRM Book Series, 464p.

Aydan, Ö. 2018. *Rock reinforcement and rock support*. CRC Press, ISRM Book Series, 486p.

Owada, Y. & Aydan, Ö. 2005. Dynamic response of fully grouted rockbolts during shaking (in Japanese). The School of Marine Science and Technology, Tokai University 3(1): 9–18.